Syn and *Anti* Aryl Nitrenium Ions

GEORGE P. FORD, P. S. HERMAN, JON W. THOMPSON

Department of Chemistry, Southern Methodist University, P.O. Box 750314, Dallas, Texas 75275

Received 10 June 1998; accepted 24 September 1998

ABSTRACT: Calculations at several levels of *ab initio* molecular orbital theory have been carried out on 20 polycyclic aryl nitrenium ions of general structure $ArNH^+$ and containing from two to four condensed rings. Electronic interactions between the aryl ring and the NH^+ group stabilize all ions relative to $PhNH^+$ by amounts varying from 14 to 40 kcal mol^{-1} depending on the ring system and on the site of substitution. Apart from a few symmetrical cases, the ions exist in distinct *syn* and *anti* configurations, separated by substantial inversion barriers. At the HF/6-31G(d) level, the latter are predicted to lie in the rather narrow range of 27.8 $\pm$ 2.0 kcal mol^{-1}. Simple PMO analyses are presented based on the analogy with odd alternant hydrocarbon cations. 1999 John Wiley & Sons, Inc. J Comput Chem 20: 231–243, 1999

Keywords: nitrenium ion; inversion barrier; *ab initio*; PMO theory

Introduction

Aryl nitrenium ions are electron-deficient divalent nitrogen species with the general formula ArN^+R. Their existence was first postulated in 1951 by Heller, Hughes, and Ingold as intermediates in the Bamberger rearrangement of *N*-hydroxyarylamines.[1] However, there was little subsequent interest in nitrenium ions until the pioneering studies of Gassman and coworkers in the 1960s, who clearly established that electron-deficient divalent nitrogen species were involved in a wide variety of ring cleavages and rearrangements in solution.[2] Although these early studies focused on aliphatic nitrenium ions, interest turned to the aryl analogs when their central role in arylamine and arylamide carcinogenesis became apparent.[3] Since then, an impressive body of evidence for the existence of aryl nitrenium ions as discrete intermediates in both the gaseous[4] and solution[5] phases has accumulated.

From a consideration of the substituent effects in the Bamberger rearrangement, Williams and coworkers concluded that the positive charge, formally associated with the nitrogen center, was largely delocalized onto the ring carbons.[6] In the language of resonance, theory this suggests a dominant role for imine-like structures (**1b**):

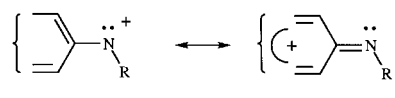

1a **1b**

Correspondence to: George P. Ford; e-mail: gford@smu.edu

CCC 0192-8651 / 99 / 020231-13

A similar conclusion was reached on the basis of semiempirical MNDO molecular orbital calculations[7] and has since been confirmed in many *ab initio* studies.[8–12] It has been suggested that this extensive delocalization of the nitrogen charge is responsible for the unexpectedly small destabilizing effect of the highly electron-withdrawing $COCH_3$ group in aryl nitrenium ions of the type ArN^+COCH_3.[8,13] The same has been suggested for the relative ease of forming ions like $ArNH_2^{2+}$ via what can be formulated as protonation of an imine-type nitrogen.[14]

The formulation of aryl nitrenium ions as imines suggests that they should exist in distinct *syn* and *anti* forms. In the course of our AM1 studies on various carbocyclic aryl nitrenium ions with R=$COCH_3$, CH_3, and H, we optimized both forms and noticed that their relative stabilities often differed by surprisingly large amounts.[9,13] Qualitative analysis of these differences suggested the presence of both steric and electronic components. Some of the largest energy differences were predicted in an AM1 study of heteroaryl nitrenium ions and attributed to the electrostatic interaction between the polar NH group and an adjacent aza substitutent.[15] Structure **2**, for example, was predicted to be 7.6 kcal mol^{-1} more stable than **3**. Even in the absence of such obvious electronic asymmetry these energy differences can amount to several kilocalories per mole. At the HF/3-21G level, structure **4** was predicted to be 3.5 kcal mol^{-1} more stable than **5**[9].

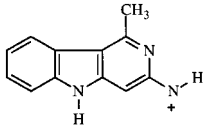

2

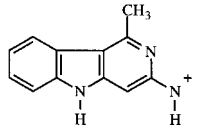

3

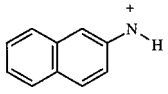

4

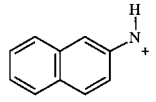

5

For many years we assumed the barrier hindering the interconversion of the alternative *syn* and *anti* forms would be very low and, therefore, the discrete existence of such forms would be of no direct relevance to nitrenium ion reactivity. However, a high-level DFT study by Cramer and coworkers[11] predicted a remarkably high barrier of 26 kcal mol^{-1} for the analogous degenerate stereomutation in the parent phenyl nitrenium ion. They also predicted the stereomutation takes place, not by rotation about the CN bond, but through a planar inversion at nitrogen in a manner similar to that recently demonstrated experimentally for neutral imines.[16] If a barrier of comparable magnitude exists in solution for the unsymmetrical nitrenium ions, there would be essentially no interconversion during their lifetimes. We became further intrigued by the likely stability of discrete configurational nitrenium ion isomers when we obtained indications that the orientation of the NH bond played a significant role in the regiochemistry of nucleophilic attack on polycyclic aryl nitrenium ions in reactions of the kind involved in covalent DNA modification.[17]

The calculations reported here were undertaken to explore the relative energies of alternative configurations of aryl nitrenium ions—and the barriers hindering their interconversion—for the complex polycyclic ions of the kind involved in DNA adduct formation.

Methods

Geometry optimizations and frequency calculations were carried out using the SPARTAN program package.[18] All optimizations were first carried out at the semiempirical AM1 level,[19] and the resulting geometries, wavefunctions, and Hessians were used as starting points in *ab initio* HF/3-21G optimizations. In a few special cases (phenyl, 9-anthryl, 2-pyrenyl) the transition state geometries for interconversion of *syn* and *anti* isomers could be obtained directly by minimizing the energy within the appropriate point group. In other cases the less stable isomer was subject to an initial constrained energy minimization (CN $\sim$1.25 Å, CNH $\sim$175°) followed by refinement to the fully optimized saddle point using SPARTAN's eigenvector-following routine. HF/6-31G(d) and MP2/6-31G(d) calculations were initiated using wave function and, where appropriate, Hessian information from lower level calculations.[20]

Vibrational analyses were carried out on all HF/3-21G structures and used to determine vibrational corrections for the computation of relative enthalpies. A scaling factor of 0.89 for the vibrational frequencies was used throughout.[21] Atomic charges based on Weinhold's natural population

analysis[22] (NPA) were obtained using routines incorporated within the SPARTAN package.

Electrostatic potential and CHELPG[23] calculations were carried out using GAUSSIAN-94.[24] Regression analyses were performed using the REG procedure of the SAS system.[25] Cited uncertainties in the regression parameters are standard errors.

Results

Energetic data for HF/6-31G(d) optimizations of the phenyl and four polycyclic nitrenium ions are shown in Table I (for structures and standard numbering see Fig. 1). Structures labeled ''*syn*'' are those in which the hydrogen of the NH group is oriented toward the β-ring carbon of higher priority in the Kahn–Ingold–Prelog sense. The alternative configurational isomers are designated ''*anti*.'' For example, **5** and **4** correspond to the *syn* and *anti* configurations of the 2-naphthyl nitrenium ion, respectively. Ions designated ''deg'' (degenerate) are those in which the two forms are symmetrically equivalent. In every case, the transition structure connecting the *syn* and *anti* configurations corresponded to an in-plane inversion at nitrogen, as found for the parent phenyl ion by Cramer and coworkers.[11]

For $PhNH^+$ the computed barrier at the MP2 level is only 1.5 kcal mol^{-1} higher than at the HF level. This suggests that electron correlation plays a rather minor role in determining the activation barriers and is consistent with the results of Cramer and coworkers.[11,26] They obtained activation barriers in the range 28.1 to 28.7 kcal mol^{-1} using Dunning's correlation-consistent polarized-valence double-ζ basis set[27] at the Hartree–Fock level and with a variety of density functional methods. Their most sophisticated DFT calculations using a triple-ζ basis set led (before application of vibrational corrections) to a barrier of 27.0 kcal mol^{-1}, which is identical to the HF/6-31G(d) value obtained here (Table I). While the precise numerical agreement is obviously fortuitous, these results strongly suggest that calculations at the relatively modest HF/6-31G(d) level provide a realistic account of the activation barriers in aryl nitrenium ions.

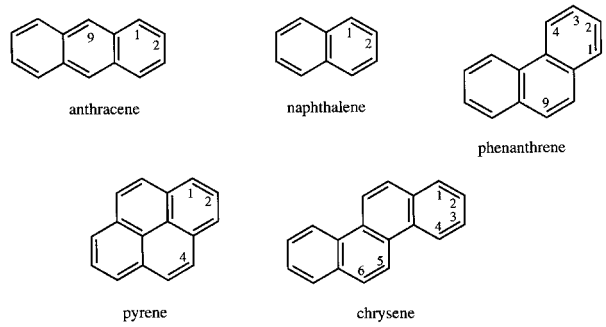

FIGURE 1. Ring systems and standard numbering of the aryl groups in $ArNH^+$.

To more fully explore these relationships the study was extended to encompass all possible substitution patterns for the five polycyclic ring systems shown in Figure 1. For practical reasons, the geometries of the energy minima and transition

TABLE I.
Energetic Data (and Hessian Indices) for Fully Optimized Structures.[a]

			HF/g-31G(d)		MP2/6-31G(d)	
Aryl	Config.	Sym.	Total energy	Relative energy	Total energy	Relative energy
Phenyl	deg	C_s	−284.85012 (0)	0.0	−285.73790	0.0
	ts	C_{2v}	−294.80708 (1)	27.0	−285.69246	28.5
1-Napthyl	*syn*	C_s	−437.52880 (0)	1.0		
	anti	C_s	−437.53046 (0)	0.0		
	ts	C_s	−437.48692 (1)	27.3		
2-Napthyl	*syn*	C_s	−437.52135 (0)	3.0		
	anti	C_s	−437.52619 (0)	0.0		
	ts	C_s	−437.47968 (1)	29.2		
9-Anthryl	deg	C_s	−590.20636	0.0		
	ts	C_{2v}	−590.16470	26.1		
2-Pyrenyl	deg	C_s	−665.93920	0.0		
	ts	C_{2v}	−665.89404	28.3		

[a]Total energies in atomic units; relative energies kilocalories per mole.

TABLE II.
Total Energies (a.u.) for HF / 3-21G-Optimized Structures.

Aryl[a]	Site	Config.[b]	Sym.	HF/3-21G		HF/6-31G(d)	MP2/6-31G(d)	E_{vib}[c]
Phenyl		deg	C_s	−283.24635	(0)	−284.84929	−285.73366	65.17
		ts	C_{2v}	−283.21366	(1)	−284.80672	—	63.81
Napthyl	1-	*syn*	C_s	−435.07047	(0)	−437.52800	−438.91841	95.41
		anti	C_s	−435.07252	(0)	−437.52956	−438.92108	95.47
		ts	C_s	−435.03925	(1)	−437.48658	—	94.06
	2-	*syn*	C_s	−435.06014	(0)	−437.52052	−438.90973	95.25
		anti	C_s	−435.06566	(0)	−437.52541	−438.91367	95.33
		ts	C_s	−435.02925	(1)	−437.47937		93.92
Anthryl	1-	*syn*	C_s	−586.87496	(0)	−590.18922		125.42
		anti	C_s	−586.87704	(0)	−590.19073	−592.08803	125.47
		ts	C_s	−586.84301	(1)	−590.14697		124.02
	2-	*syn*	C_s	−586.86298	(0)	−590.18088		125.22
		anti	C_s	−586.87005	(0)	−590.18697	−592.08032	125.34
		ts	C_s	−586.83205	(1)	−590.13951		123.89
	9-	deg	C_s	−586.89507	(0)	−590.20550	−592.10388	125.76
		ts	C_{2v}	−586.86387	(1)	−590.16436		124.30
Phenanthryl	1-	*syn*	C_s	−586.87060	(0)	−590.18357		125.43
		anti	C_s	−586.87547	(0)	−590.18784	−592.08669	125.54
		ts	C_s	−586.84039	(1)	−590.14312		124.09
	2-	*syn*	C_s	−586.86601	(0)	−590.18203		125.43
		anti	C_s	−586.86866	(0)	−590.18437	−592.07978	125.46
		ts	C_s	−586.83312	(1)	−590.13898		124.08
	3-	*syn*	C_s	−586.86988	(0)	−590.18594		125.37
		anti	C_s	−586.87383	(0)	−590.18950	−592.08484	125.43
		ts	C_s	−586.83752	(1)	−590.13449		124.04
	4-	*syn*	C_1	−586.86272	(0)	−590.17629		125.30
		anti	C_s	−586.86629	(0)	−590.17831	−592.07828	125.51
		ts	C_1	−586.82978	(1)	−590.13296		123.95
	9-	*syn*	C_s	−586.87851	(0)	−590.19140	−592.08732	125.60
		anti	C_s	−586.87569	(0)	−590.18859		125.57
		ts	C_s	−586.84434	(1)	−590.14716		124.16
Pyrenyl	1-	*syn*	C_s	−662.22490	(0)	−665.96650		133.77
		anti	C_s	−662.23203	(0)	−665.97242		133.87
		ts	C_s	−662.84434	(1)	−665.92620		132.41
	2-	deg	C_s	−662.19407	(0)	−665.93838		133.41
		ts	C_{2v}	−662.15951	(1)	−665.89370		132.06
	4-	*syn*	C_s	−662.21303	(0)	−665.95402		133.69
		anti	C_s	−662.21008	(0)	−665.95116		133.64
		ts	C_s	−662.17861	(1)	−665.90954		132.27
Chrysenyl	1-	*syn*	C_s	−738.67130	(0)	−742.83981		155.56
		anti	C_s	−738.67537	(0)	−742.84322		155.63
		ts	C_s	−738.64035	(1)	−742.79852		154.16
	2-	*syn*	C_s	−738.66566	(0)	−742.83750		155.56
		anti	C_s	−738.66924	(0)	−742.84059		155.60
		ts	C_s	−738.63289	(1)	−742.79445		154.21
	3-	*syn*	C_s	−738.66791	(0)	−742.83966		155.38
		anti	C_s	−738.67292	(0)	−742.84410		155.46
		ts	C_s	−738.63581	(1)	−742.79727		154.06
	4-	*syn*	C_1	−738.66497	(0)	−742.83383		155.44
		anti	C_s	−738.66711	(0)	−742.83453		155.67
		ts	C_1	−738.63083	(1)	−742.78948		154.01

TABLE II.
(Continued)

Aryl[a]	Site	Config.[b]	Sym.	HF/3-21G		HF/6-31G(d)	MP2/6-31G(d)	E_{vib}[c]
	5-	*syn*	C_1	−738.66757	(0)	−742.83639		155.48
		anti	C_s	−738.66339	(0)	−742.83152		155.65
		ts	C_1	−738.63024	(1)	−742.78905		154.09
	6-	*syn*	C_s	−738.68546	(0)	−742.85392		155.73
		anti	C_s	−738.68408	(0)	−742.85234		155.70
		ts	C_s	−738.65136	(1)	−742.80963		154.32

[a] See Figure 1 for structures and numbering.
[b] Designations *syn* and *anti* refer to the orientation of the NH bond (see text). The designated ''deg'' indicates that the *syn* and *anti* configurations are symmetrically equivalent.
[c] Sum of zero-point energy and vibrational enthalpies at 298° K (kcal mol^{-1}) from scaled HF/3-21G vibrational frequencies.

states were computed at the more economical HF/3-21G level with selected single-point calculations at the higher levels. The total energies are collected in Table II together with the (HF/3-21G) vibrational contributions to the enthalpy. All ions were found to have planar C_s or C_{2v} structures with the exception of the highly congested *syn* configurations of the bay-region ions (4-phenanthryl, 4-chrysenyl, and 5-chrysenyl) and the transition states involving them.

The relative abilities of different aryl groups to stabilize the corresponding nitrenium ions, ΔH_{stab}, were quantified through the enthalpy changes for the isodesmic relationship in eq. (1). A positive value corresponds to the amount by which the nitrenium ion, $ArNH^+$ is more stable than $PhNH^+$.

$$Ph—H + Ar—NH^+ \rightarrow Ar—H + Ph—NH^+ \quad (1)$$

$$Ph—H + Ar—CH_2^+ \rightarrow Ar—H + Ph—CH_2^+ \quad (2)$$

The computed values, based on HF/3-21G-optimized geometries and vibrational corrections (and data for the parent arenes in Table III), are summarized in Table IV. In all cases, ΔH_{stab} refers to the more stable of the *syn* and *anti* isomers. For comparison, the analogous quantities for the benzylic ions, $ArCH_2^+$, computed from eq. (2), are also included in Table III. With the exception of the 9-anthryl and bay-region ions (4-phenanthryl, 4-chrysenyl, and 5-chrysenyl), all were computed to have planar C_s or C_{2v} structures.[28]

The general pattern of varying nitrenium ion stabilities is very similar to that predicted in the earlier semiempirical AM1 calculations.[9] The *ab initio* stabilization energies are generally larger than those predicted by AM1 and increase in the order HF/3-21G < HF/6-31G(d) < MP2/6-31G(d). However, the results of all four methods are closely correlated with one another ($r \geq 0.99$ for all pairs).

Table V summarizes additional data that relate directly to the question of the extent to which aryl nitrenium ions are better described as imino carbenium ions. The charges, q_N, q_{NH}, and q_N^{π}, refer to the total charge associated with the nitrogen atom, the charge associated with the NH group, and the

TABLE III.
Total Energies (a.u.) for HF/3-21G-Optimized Structures.

Arene	HF/3-21G	HF/6-31G(d)	MP2/6-31G(d)	E_{vib}[a]
Benzene (D_{6h})	−229.41945	−230.70307	−231.45589	61.80
Napthalene (D_{2h})	−381.21581	−383.35494	−384.61104	91.67
Anthracene (D_{2h})	−533.00347	−535.99864	−537.75984	121.47
Phenanthrene (C_{2v})	−533.01572	−536.00962	−537.77086	121.75
Pyrene (D_{2h})	−608.34759	−611.76782		129.83
Chrysene (C_{2h})	−684.81179	−688.66072		151.90

[a] See footnote c from Table II.

TABLE IV.
Stabilities of Nitrenium and Carbenium Ions Relative to Phenyl Analogs (kcal mol^{-1}).[a]

			$ArNH^+$			$ArCH_2^+$
Aryl	Site	Config.[b]	HF/3-21G	HF/6-31G(d)	MP2/6-31G(d)	HF/6-31G(d)
Phenyl		deg	0.0	0.0	0.0	0.0
Naphthyl	1-	*anti*	18.3	17.4	19.8	8.3
	2-	*anti*	14.1	14.9	15.3	8.3
Anthryl	1-	*anti*	28.7	28.2	31.0	14.9
	2-	*anti*	24.4	25.9	26.3	14.9
	9-	deg	39.7	37.2	40.7	20.4
Phenanthryl	1-	*anti*	20.2	19.4	23.5	8.9
	2-	*anti*	16.0	17.6	19.2	10.6
	3-	*anti*	19.3	20.9	22.4	12.2
	4-	*anti*	14.5	13.7	18.2	3.8
	9-	*syn*	22.0	21.1	23.8	10.9
Pyrenyl	1-	*anti*	36.5	35.9		20.7
	2-	deg	13.2	15.1		9.5
	4-	*syn*	24.8	24.6		12.4
Chrysenyl	1-	*anti*	22.6	22.4		10.8
	2-	*anti*	18.9	20.8		12.4
	3-	*anti*	21.3	23.1		13.4
	4-	*anti*	17.4	16.9		6.3
	5-	*syn*	19.9	18.3		6.7
	6-	*syn*	28.8	29.0		15.9

[a]Computed from eq. (1) or eq. (2), including vibrational corrections. All energies obtained using HF/3-21G-optimized geometries.
[b]Configuration of the more stable nitrenium ion used in the calculation.

TABLE V.
Computed Data for $ArNH^+$ (HF/3-21G Geometries).[a]

Aryl	Position	Config.	q_N[a]	q_{NH}	q_N^π	r_{CN}[b]	ν_{CN}[c] ($\Delta\nu_{CN}$)[d]
Phenyl		deg	−0.363	0.043	0.156	1.273	1543 (12)
Napthyl	1-	*anti*	−0.484	−0.086	0.017	1.263	1612 (11), 1567 (6)
	2-	*anti*	−0.449	−0.049	0.060	1.269	1585 (8), 1550 (6)
Anthryl	1-	*anti*	−0.547	−0.157	−0.057	1.262	1630 (11), 1573 (5)
	2-	*anti*	−0.510	−0.116	−0.010	1.267	1600 (9), 1550 (5)
	9-	deg	−0.562	−0.173	−0.076	1.257	1639 (16)
Phenanthryl	1-	*anti*	−0.499	−0.102	0.004	1.263	1620 (6)
	2-	*anti*	−0.458	−0.062	0.046	1.268	1571 (10)
	3-	*anti*	−0.481	−0.086	0.023	1.267	1587 (10)
	4-	*anti*	−0.504	−0.107	0.002	1.263	1582 (8)
	9-	*syn*	−0.498	−0.104	−0.001	1.266	1600 (13)
Pyrenyl	1-	*anti*	−0.547	−0.154	−0.050	1.261	1642 (7), 1601 (9)
	2-	deg	−0.444	−0.050	0.061	1.270	1567 (11)
	4-	*syn*	−0.518	−0.127	−0.025	1.265	1602 (10), 1579 (6)
Chrysenyl	1-	*anti*	−0.515	−0.121	−0.016	1.263	1625 (8), 1586 (9)
	2-	*anti*	−0.477	−0.083	0.025	1.267	1560 (5)
	3-	*anti*	−0.494	−0.100	0.008	1.267	1589 (11)
	4-	*anti*	−0.523	−0.129	−0.022	1.267	1617 (5), 1587 (12)
	5-	*syn*	−0.502	−0.099		1.269	1585 (7), 1564 (7)
	6-	*syn*	−0.526	−0.137	−0.035	1.264	1612 (15)

[a]NPA charges, q_N, q_{NH}, q_N^π, from the HF/6-31G(d) wave functions.
[b]CN bond distance (Å).
[c]Frequency (cm^{-1}) of vibrations with significant ν_{CN} character. Values are corrected HF/3-21G data (see text).
[d]Isotopic shift to lower frequency on ^{15}N substitution. Data are included for all vibrations for which $\Delta\nu \geq 5$ cm^{-1}.

nitrogen "π-charge," respectively. All are NPA charges based on the 6-31G(d) wave functions. The CN distances and vibrational frequencies refer to the HF/3-21G geometries.

No experimental data are yet available for bond distances in aryl nitrenium ions of this general structure. However, the CN distances in various keto imines **6a**, for which nitrenium ion-like resonance structures can be written, fall[29] in the range 1.300 ± 0.006. This is similar to the 1.288 Å predicted in Cramer's DFT study of $PhNH^+$.[11] The HF method systematically underestimates bond distances.[30] For the HF/3-21G values reported in Table V the errors are expected to be about 2% to 4% [e.g., $r_{CN}(PhNH^+)$ = 1.273 Å; r_{CN}(**6b**) = 1.262 Å].

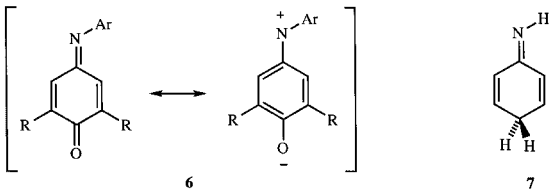

6

a: Ar = various aryl, R = *t*-Bu **b**: Ar = Ph, R = H

7

The unambiguous assignment of a unique CN stretching vibration in many of the nitrenium ions was complicated by strong in-phase and out-of-phase coupling with ring stretching and ring breathing modes. To solve this problem we imposed the arbitrary criterion that only vibrations shifted by ≥ 5 cm^{-1} on ^{15}N substitution were considered to have sufficient CN stretching character for inclusion in Table V.

To assist in interpreting these data we also carried out analogous calculations on the "genuine" imine, **7** (see Fig. 2). Like the aryl nitrenium ions, **7** is also predicted to undergo stereomutation via in-plane nitrogen inversion. At the HF/6-31G(d)//HF/3-21G level, $\Delta H^{\ddagger}$ is predicted to be 31.0 kcal mol^{-1}.

The computed enthalpy changes, ΔH, and the activation enthalpies, $\Delta H^{\ddagger}$, for conversion from the more stable to the less stable nitrenium ion configurations are summarized in Table VI. The majority of the data refer to single-point HF/6-31G(d)//HF/3-21G calculations. Comparison with the five cases where fully optimized structures were obtained suggests that the single-point approximation does not introduce serious errors into the relative energies.

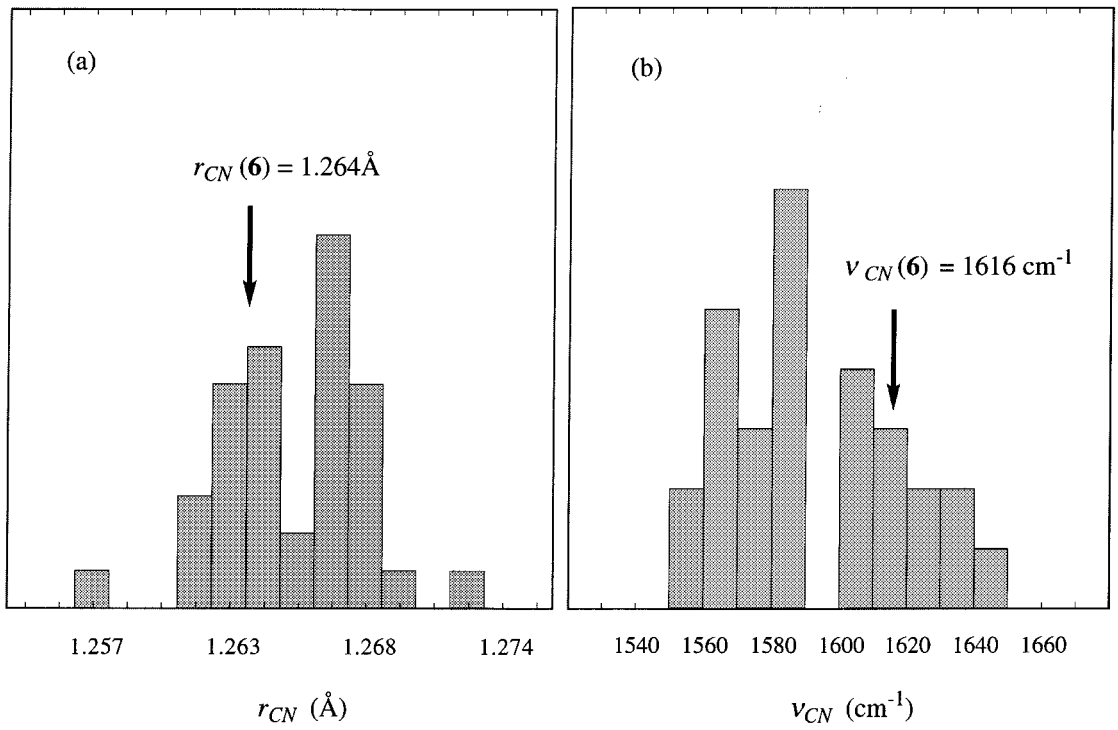

FIGURE 2. Distribution of HF/3-21G aryl nitrenium ion (a) CN bond lengths, r_{CN}, and (b) stretching frequencies, ν_{CN}. For comparison, the analogous quantities for the imine **6** are indicated in each panel.

TABLE VI.
Computed [HF/6-31G(d)] Values of ΔH and $\Delta H^{\ddagger}$ for Interconversion of *Syn* and *Anti* Aryl Nitenium Ions (kcal mol^{-1}).[a]

Aryl	Site	Process	ΔH		$\Delta H^{\ddagger}$	
			Single point	Fully optimized	Single point	Fully optimized
Phenyl		deg	0.0	0.0	25.3	25.6
Naphthyl	1-	*anti* → *syn*	0.9	1.0	25.6	25.9
	2-	*anti* → *syn*	3.0	3.0	27.5	27.8
Anthryl	1-	*anti* → *syn*	0.9		26.0	
	2-	*anti* → *syn*	3.7		28.3	
	9-	deg	0.0	0.0	24.3	24.7
Phenanthryl	1-	*anti* → *syn*	2.6		26.6	
	2-	*anti* → *syn*	1.4		27.1	
	3-	*anti* → *syn*	2.2		27.5	
	4-	*anti* → *syn*	1.1		26.9	
	9-	*syn* → *anti*	1.7		26.4	
Pyrenyl	1-	*anti* → *syn*	3.6		27.5	
	2-	deg	0.0	0.0	26.6	26.9
	4-	*syn* → *anti*	1.7		26.5	
Chrysenyl	1-	*anti* → *syn*	2.1		26.5	
	2-	*anti* → *syn*	1.9		27.6	
	3-	*anti* → *syn*	2.7		28.0	
	4-	*anti* → *syn*	0.2		26.6	
	5-	*syn* → *anti*	3.2		28.3	
	6-	*syn* → *anti*	1.0		26.4	

[a]Based on data in Table II including vibrational corrections. Single-point calculations refer to HF/3-21G geometries.

Discussion

STRUCTURES AND STABILITIES OF ARYL NITRENIUM IONS

The relative stabilities of aryl nitrenium ions, ΔH_{stab}, vary markedly with the nature of the aryl group. At the highest level studied (MP2/6-31G(d)//HF/3-21G) they are predicted to span a remarkable 40 kcal mol^{-1}. These variations largely reflect the differing abilities of the aryl moieties to delocalize electron density onto the formally positive NH group. Indeed, a simple semiquantitative model based on AM1 results was formulated[9] on this basis using the ideas of PMO theory.

A survey of the data in Table V reinforces this conclusion. A striking feature of these results is that the nitrogen charges, q_N, are large and *negative*. A similar phenomenon was observed in Mulliken population analyses of some of the same ions at the HF/3-21G level.[9] However, the impact of those results was tempered by the well-known shortcomings of the Mulliken analysis. In both cases, the reasons can be traced partly to the substantial migration of electron density along the NH bond. Even when the NH group is considered as a single entity, its overall charge, q_{NH}, is positive only for $PhNH^+$. The π-component of the charge, q_N^{π}, is of special interest in connection with the resonance description of nitrenium ions. This is modestly positive for $PhNH^+$, but close to zero (-0.007 ± 0.069) for the remaining ions. Taken together, these results are far more consistent with the representation of aryl nitrenium ions as imino carbenium ions (**1b**) rather than as derivatives of H_2N^+.

A similar picture emerges from the computed distances (r_{CN}) and stretching frequencies (ν_{CN}). The former cluster around a median value of 1.266 Å, which is only slightly longer than the 1.264 Å computed for **7** (Fig. 2a) and much shorter than the 1.376 Å computed for aniline.[31] Similarly, the ν_{CN} data cluster around 1587 cm^{-1}, which is slightly lower than the 1616 cm^{-1} in **7** (Fig. 2b). Typical CN stretching frequencies in primary aromatic amines fall in the range 1315 ± 65 cm^{-1}.[32] No experimental IR data have yet been reported for primary aryl nitrenium ions. However, Toscano and coworkers[33] obtained a partial IR spectrum for

an acrylonitrile solution of Ph_2N^+ in which a band at 1392 cm^{-1} (1376 cm^{-1} in the ^{15}N isomer) was identified as ν_{CN}. This can be expected to occur at substantially lower frequencies than those predicted for ions of the type $ArNH^+$ because only one of the two CN bonds in structures like **1b** is double. Nevertheless, it is significant that it was observed at a higher frequency than the analogous vibration in diphenylamine.[33]

Because of their generally smaller size, alkyl nitrenium ions have been studied at far higher levels of DFT and *ab initio* theory than is currently possible for many of the systems considered here (see, e.g., Gonzales et al.[34]). These results can be of interest in their own right. However, it is worth emphasizing that, for reasons just discussed, simple alkyl nitrenium ions are poor models for the kinds of ions studied here, namely those implicated in aryl amine and amide carcinogenesis.

RELATIVE STABILITIES OF *SYN* AND *ANTI* NITRENIUM IONS

Close inspection of the energy differences between the *syn* and *anti* nitrenium ion configurations reveals some surprises (Table VI). In each case, the data refer to the ''uphill'' conversion ($\Delta H \geq 0$). That **8** is less stable than **9** seems consistent with the presence of a peri interaction in the former. This cannot be the only factor involved because the stabilities of **4** and **5**, where no peri interactions are present, differ by three times as much. More surprisingly, the stable isomer of the 9-phenanthryl nitrenium ion has the sterically congested *syn* configuration (**10**). A similar situation exists for 4-pyrenyl and 6-chrysenyl ions. Most strikingly, the stable configuration of the 5-chrysenyl ion (**11**) is one in which the NH bond lies in the bay region—a configuration so congested that the molecule is forced into an atypical nonplanar C_1 structure:

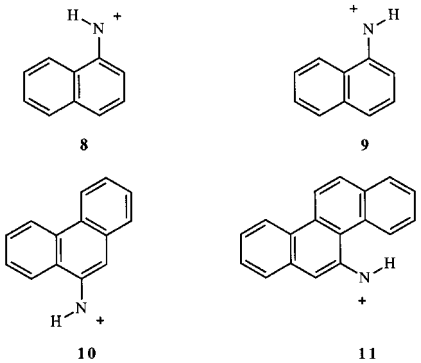

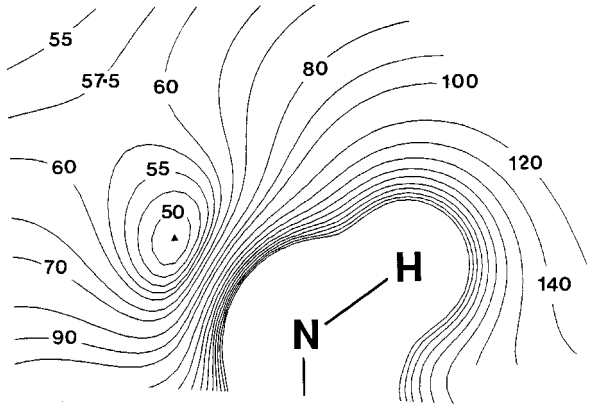

FIGURE 3. The HF/6-31G(d) electrostatic potential (kcal mol^{-1}) in the molecular plane of $PhNH^+$. CHelpG charges: $q_H = 0.381$; $q_N = -0.130$; $q_{LP} = -0.052$.

The second factor involved in the differential stabilization of the alternative configurations is related to the high electrostatic asymmetry of the NH bond. This asymmetry is clearly apparent in the electrostatic potential around the NH group of the phenyl nitrenium ion and in the corresponding CHELPG analysis (Fig. 3). In the latter, the effective lone pair charge, q_{LP}, was represented by a ghost atom at the minimum in the electrostatic potential. Electrostatic interactions between the NH group and the aryl core favor the configuration in which the nitrogen lone pair is directed toward, and the NH bond away from, nearby regions of high positive charge. We shall return to this point in the last section.

INTERCONVERSION OF *SYN* AND *ANTI* IONS

The nature of the aryl group has very little effect on the computed inversion barriers, $\Delta H^{\ddagger}$ (Table VI). For example, differences in the electronic interactions between the NH groups and the aryl rings in the phenyl and 9-anthryl ions stabilize the latter by 37 to 40 kcal mol^{-1}; however, the computed $\Delta H^{\ddagger}$ values differ by less than 1 kcal mol^{-1}. The values of $\Delta H^{\ddagger}$ in Table VI span a mere 4 kcal mol^{-1}. These variations are entirely unrelated to the overall electronic interaction with the ring as reflected in either q_N^{π} or ΔH_{stab} ($r^2 = 0.031$ and 0.000, respectively). Instead, they appear to reflect variations in ΔH and differences in the relief of steric strain on linearization of the CNH bond angle in the transition state. These factors can be approximately quantified in terms of the multi-

ple regression equation:

$$\Delta H^{\ddagger} = 26.134(\pm 0.197) + 0.603(\pm 0.148)\Delta H - 0.833(\pm 0.148)(I_s + I_t) \quad (3)$$
$$(r^2 = 0.896,\ p = 0.0001,\ n = 17)$$

Here, I_s and I_t are indicator variables that refer to the two β-ring carbons and are assigned a value of $+1$ if the carbon atom is a point of ring fusion and zero if it is not. Thus, the quantity $I_s + I_t$ takes the values 0, 1, or 2, depending on the total number of peri interactions eliminated on forming the transition state. All terms in eq. (3) were significant at the $p \leq 0.0001$ level. Interestingly, the bay-region ions, which were excluded in the development of eq. (3), also follow this relationship rather closely (Fig. 4).

INSIGHTS FROM PMO THEORY

The relative stabilities of the aryl nitrenium ions, ΔH_{stab}, approximately parallel the analogous quantities for the benzylic ions but are about twice as large. In other words, electron delocalization by a given aryl group stabilizes the nitrenium ion about twice as effectively as it does the carbenium ion. This was noted in our earlier AM1 study and is a consequence of the electronegativity difference between carbon and nitrogen.[9]

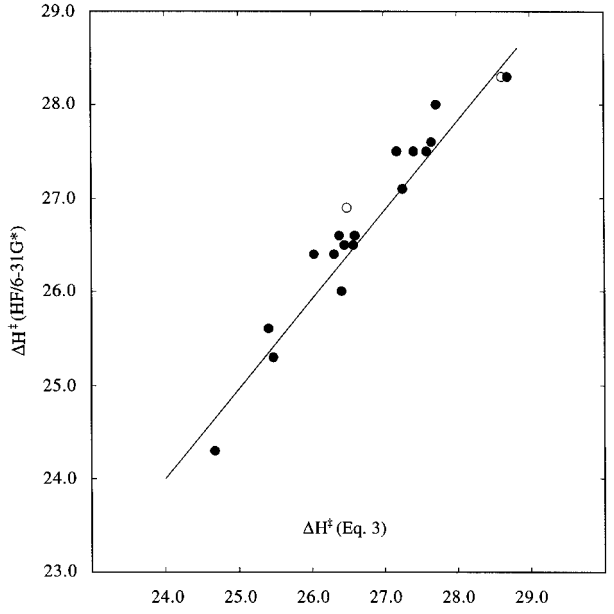

FIGURE 4. Comparison of the activation barriers for nitrogen inversion in $ArNH^+$ computed directly [HF/6-31G(d) // HF/3-21G] with those given by eq. (3). Bay-region compounds, indicated by open circles, were not used in the development of the regression.

In a recent DFT study, Cramer et al.[35] found that markedly different chemical and electronic properties were predicted for the isoelectronic species, PhXMe ($X = B^-$, C, N^+). This was attributed to differences in the formal charge associated with X. In contrast, the isoelectronic analogy between the singly cationic nitrenium and benzylic ions appears to be a very useful one. We show that simple PMO theory, which strictly applies to the benzylic ions, provides powerful and convenient qualitative insights into arylnitrenium ion behavior predicted by the *ab initio* calculations.

At the level of simple Huckel π-electron theory the nitrenium and benzylic ions are related through a change in the coulomb integral of the exocyclic atom from α to $\alpha + h_N\beta$. The corresponding first-order change in the π-energy is $\sim h_N\beta Q^{\pi}$, where Q^{π} is the π-electron population at the specified position of the benzylic ion. From the properties of odd alternant hydrocarbons, the latter is just $1 - a_0^2$, where a_0 is the coefficient of the nonbonding orbital.[36] These coefficients are easily obtained in simple pencil-and-paper calculations using the ''starring'' procedure. Application of this simple treatment to the data in Table VI is shown in Figure 5, which corresponds to the regression equation:

$$\Delta H_{stab}(Ar{-}NH^+) = \Delta H_{stab}(Ar{-}CH_2^+) + h_N\beta\left[a_0^2(Ar) - a_0^2(Ph)\right] + C \quad (4)$$
$$(h_N\beta = -45.52 \pm 5.17,\ C = 5.31 \pm 0.65,\ r^2 = 0.812,\ p = 0.0001,\ n = 20)$$

This equation quantifies the intuition that, for a given aryl group, the nitrenium ion enjoys a stabilization beyond that in the analogous benzylic ion, and that this stabilization increases as the π-charge at the exocyclic atom decreases. Although phenyl is an obvious outlier, the quality of the relationship is surprisingly high.

The PMO framework also leads to a simple qualitative understanding of the relative stabilities of the *syn* and *anti* configurations of individual nitrenium ions. Because the change in α leads to no first-order change in the wave function, the charge distributions in the nitrenium ions should be qualitatively similar to those in the alternant hydrocarbon. The Hückel π-charges computed in this way for the 9-phenanthryl ion are shown in what follows. In the preferred configuration (shown) the hydrogen atom is oriented toward the

β-carbon bearing the smaller positive charge (a_0^2 = 1/56 vs. 16/56):

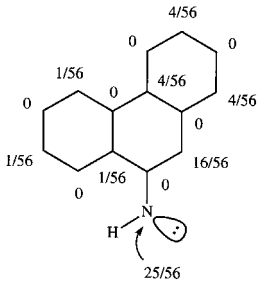

Because the π-charge distribution is determined solely by the coefficients of a nonbonding orbital, the only nonzero ring charges in the immediate vicinity of the NH group are located at the two β-carbons. This suggests a simple four-point electrostatic model for the interaction between the NH group and the aryl moiety (Fig. 6) that leads to eq. (5):

$$\Delta E = (q_t - q_s)\left\{\frac{q_H(R_t - R_s)}{R_t R_s} + \frac{q_{LP}(r_t - r_s)}{r_t r_s}\right\} \quad (5)$$

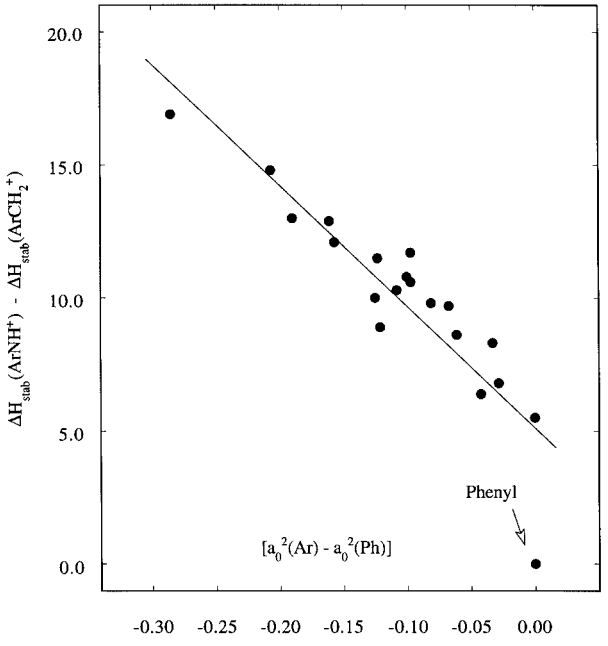

FIGURE 5. Parallel between the additional stabilizing ability of Ar in $ArNH^+$ (compared with $ArCh_2^+$) and the Huckel π-charge on the exocyclic atom as given by a_0^2. See eq. (4).

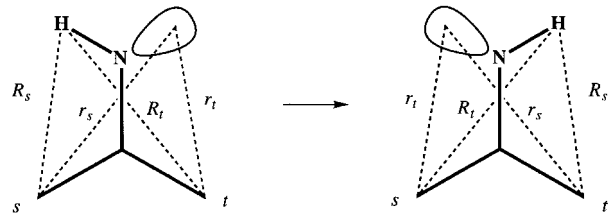

FIGURE 6. Four-point model for the electrostatic interaction between an NH group and the β-ring carbons in $ArNH^+$. Atomic charges, q_H and q_{LP}, are located on the hydrogen atom and within the lone pair. Charges at the two ring carbons are designated q_s and q_t.

If the term in curly brackets is reasonably insensitive to the identity of Ar,[37] the electrostatic contribution to the difference in stability between the two configurations should be approximately proportional to $a_{0t}^2 - a_{0s}^2$. That this is qualitatively true is shown in Figure 7, which portrays the quality of the least-squares fit of the HF/6-31G(d)//HF/6-31G values of ΔH to eq. (6). In this equation, I_s and I_t are indicator variables describing the number of peri interactions analogous to those used earlier:

$$\Delta H = 17.81(\pm 1.17)\left[\alpha_{0t}^2 - \alpha_{0s}^2\right] + 3.69(\pm 0.27)[I_t - I_s] \quad (6)$$
$$(r^2 = 0.936,\ n = 17,\ p = 0.0001)$$

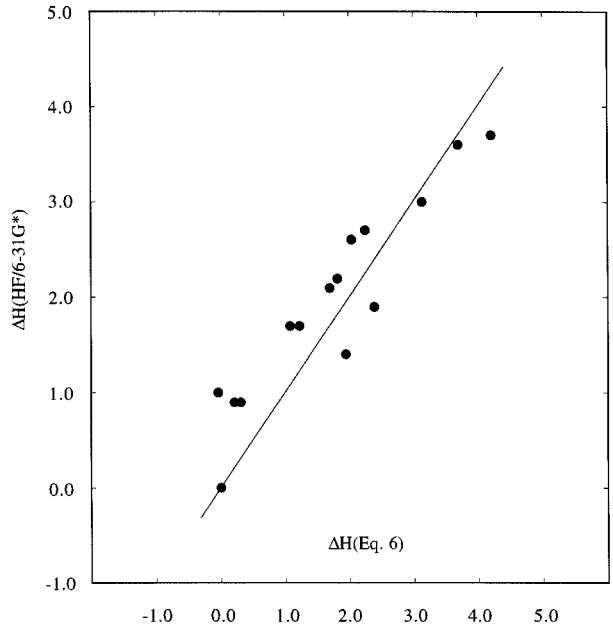

FIGURE 7. Comparison of the computed relative energies of the *syn* and *anti* nitrenium ion configurations with those given by eq. (6).

They are assigned the value +1 if the designated atom is a point of ring fusion, and zero otherwise. Thus, the quantity $I_t - I_s$ takes values +1, 0, or −1 corresponding to the number of peri interactions created on nitrogen inversion.

Conclusions

Nitrenium ions of general structure $ArNH^+$ are stabilized by amounts that vary widely with the nature of the aryl group. This effect is far more pronounced than for the benzylic analogs, due to the stabilizing effect of delocalizing electron density onto the more electronegative NH (rather than) CH_2 group. For the phenyl and, especially, the more complex aryl, nitrenium ions the electronic interaction between the aryl and NH groups is sufficiently complete that the computed structural features of the CN linkage are those of imines and bear little resemblance to properties expected for derivatives of H_2N^+. The computed CN distances and vibrational frequencies are similar to those in a neutral conjugated imine. The π-charges are little different from zero. Like imines, the nitrenium ions exist in distinct *syn* and *anti* configurations that interconvert via nitrogen inversion. The relative stabilities of the two configurations are determined by a combination of steric effects and the electrostatic interaction between the NH group and the positive charge distribution in the ring. Activation barriers separating the *syn* and *anti* configurations are quite high and vary little (27.8 ± 2.0 kcal mol^{-1}).

References

1. Heller, H. E.; Hughes, E. D.; Ingold, C. K. Nature 1951, 168, 910.
2. Gassman, P. G. Acc Chem Res 1970, 26, 26.
3. For reviews, see: Neuman, H.-G. J Cancer Res Clin Oncol 1986, 112, 100; Beland, F. A.; Kadlubar, F. F. Environ Health Perspect 1985, 62, 19; Garner, R. C.; Martin, C. N.; Clayson, D. B. In Chemical Carcinogens; Searle, C. E., Ed. (ACS Symposium Series 182, Vol 1) American Chemical Society: Washington, DC, 1984; Miller, J. A.; Miller, E. C. Environ Health Perspect 1983, 49, 3; Kriek, E.; Westra, J. G. In Chemical Carcinogens and DNA; Grover, P. L. Ed. Vol 2. CRC Press: Boca Raton, FL, 1979.
4. Attina, M.; Cacace, F.; DePetris, G.; Grandinetti, F. Int J Mass Spect Ion Proc 1989, 90, 263.
5. Davidse, P. A.; Kahley, M. J.; McClelland, R. A.; Novak, M. J Am Chem Soc 1997, 116, 4513; Robbins, R. J.; Laman, D. M.; Falvey, D. M. 1996, 118, 8127; McClelland, R. A. Tetrehedron 1996, 52, 6823; Rieker, A.; Speiser, B. Tetrahed Lett 1990, 31, 5013; Fishbein, J. C.; McClelland, R. A. J Am Chem Soc 1987, 109, 2824.
6. Kohnstam, G.; Petch, W. A.; Williams, D. L. H. JCS Perkin Trans 1984, 2, 423; Williams, D. L. H; Buncel, E. Isotopes in Organic Chemistry, Vol 5, Buncel, E.; Lee, C. E., Ed. Elsevier: Amsterdam, 1980.
7. Ford, G. P.; Scribner, J. D. J Am Chem Soc 1981, 103, 4281.
8. Ford, G. P.; Herman, P. S. J Mol Struct (Theochem) 1990, 204, 121.
9. Ford, G. P.; Herman, P. S. J Mol Struct (Theochem) 1991, 236, 269.
10. Li, Y.; Abramovich, R. A.; Houk, K. N. J Org Chem 1989, 54, 2911; Ohwada, T.; Shudo, K. J Am Chem Soc 1989, 111, 34.
11. Cramer, C. J.; Dulles, F. J.; Falvey, D. E. J Am Chem Soc 1994, 116, 9787.
12. Novak, M.; Kahley, M. J.; Lin, J.; Kennedy, S. A.; Swanegan, L. A. J Am Chem Soc 1994, 116, 11626.
13. Ford, G. P.; Herman, P. S. J Chem Soc Perkin Trans 1991, 2, 607.
14. McClelland, R. A.; Kahley, M. J.; Davidse, P. A.; Hadzialic, G. J Am Chem Soc 1996, 118, 4794.
15. Ford, G. P.; Griffin, G. R. Chem-Biol Interact 1992, 81, 19.
16. Guerra, A.; Lunazzi, L. J Org Chem 1995, 60, 7959. See also: Jennings, W. B.; Wilson, V. E. In Acyclic Organonitrogen Stereodynamics; Lambert, J. B.; Takeuchi, Y., Eds. VCH: New York, 1992; Bach, R. D.; Raban, M. In Cyclic Organonitrogen Stereodynamics; Lambert, J. B.; Takeuchi, Y., Eds. VCH: New York, 1992.
17. Ford, G. P.; Thompson, J. W. Chem Res Toxicol 1999, in press.
18. SPARTAN, versions 3 and 4, Wavefunction, Inc, 18401 Von Karman Avenue, Suite 370, Irvine, CA 92612.
19. Dewar, M. J. S.; Zoebisch, E. G.; Healy, E. F.; Stewart, J. J. P. J Am Chem Soc 1985, 107, 3902.
20. Basis sets, HF/3-21G: Binkley, J. S.; Pople, J. A.; Hehre, W. J. J Am Chem Soc 1980, 102, 939; 6-31G(d): Hariharan, P. C.; Pople, J. A. Chem Phys Lett 1972, 66, 217.
21. Pople, J. A.; Schlegel, H. B.; Krishnan, P.; DeFrees, D. J.; Binkley, J. S.; Frisch, M. J.; Whiteside, R. A.; Hout, R. F.; Hehre, W. J. Int J Quantum Chem QBS 1981, 15, 269.
22. Reed, A. E.; Curtiss, L. A.; Weinhold, F. Chem Rev 1988, 88, 735.
23. Breneman, C. M.; Wiberg, K. B. J Comput Chem 1990, 11, 361.
24. Frisch, M. J.; Trucks, G. W.; Schlegel, H. B.; Gill, P. M. W.; Johnson, B. G.; Robb, M. A.; Cheeseman, J. R.; Keith, T.; Petersson, G. A.; Montgomery, J. A.; Raghavachari, K.; Al-Laham, M. A.; Zakrzewski, V. G.; Ortiz, J. V.; Foresman, J. B.; Cioslowski, J.; Stefanov, B. B.; Nanayakkara, A.; Challacombe, M.; Peng, C. Y.; Ayala, P. Y.; Chen, W.; Wong, M. W.; Andres, J. L.; Replogle, E. S.; Gomperts, R.; Martin, R. L.; Fox, D. J.; Binkley, J. S.; Defrees, D. J.; Baker, J.; Stewart, J. P.; Head-Gordon, M.; Gonzalez, C.; Pople, J. A. GAUSSIAN-94 (Revision D.4), Gaussian, Inc., Pittsburgh, PA, 1995.
25. The SAS System, (Version 6.12), SAS Institute, Cary, NC, 1996.
26. Cramer, C. J.; Dulles, F. J.; Falvey, D. E. Supplementary data to ref. 11.
27. Dunning, T. H. J Chem Phys 1989, 90, 107.

28. In the interests of brevity, the details of these calculations are not reported; however, they may be obtained from the authors on request.
29. Based on 13 examples in the Cambridge Structural Database: Allen, F. H.; Kennard, O. Chemical Design Automation News 1993, 8, 31.
30. Hehre, W. J.; Radom, L.; Schleyer, P. v. R.; Pople, J. A. In Ab Initio Molecular Orbital Theory. John Wiley & Sons: New York, 1986, 146.
31. Experimental value is 1.402 Å: Niu, Z.; Boggs, J. E. Theochem, 1984, 109, 381.
32. Cross, A. D.; Jones, R. A. An Introduction to Practical Infra-Red Spectroscopy; Butterworths: London, 1969.
33. Srivastava, S.; Toscano, J. P.; Moran, R. J.; Falvey, D. E. J Am Chem Soc 1997, 119, 11552.
34. Gonzales, C.; Restrepo-Cossio, A.; Márquez, M.; Wiberg, K. B.; DeRosa, M. J Phys Chem A 1998, 102, 2732.
35. Cramer, C. J.; Truhlar, D. G. J Am Chem Soc 1997, 119, 12338.
36. For a comprehensive description of PMO theory and its applications in organic chemistry see: Dewar, M. J. S.; Dougherty, R. C. The PMO Theory Organic Chemistry; Plenum Press: New York, 1975.
37. That this is likely to be true can be seen, for example, in the NPA values of q_H (equal to $q_{NH} - q_N$ in Table VI), which fall in the very narrow range of 0.398 ± 0.009.